Chapter 1

SPECTRAL PROPERTIES OF UNDERDOPED CUPRATES

A. Ramšak[1,2], P. Prelovšek[1,2], and I. Sega[1]
[1] *J. Stefan Institute, SI-1000 Ljubljana, Slovenia*
[2] *Faculty of Mathematics and Physics, University of Ljubljana, SI-1000 Ljubljana, Slovenia*

Abstract In the framework of the planar t-J model for cuprates we analyze the development of a pseudo gap in the density of states, which at low doping starts to emerge for temperatures $T < J$ and persists up to the optimum doping. The analysis is based on numerical results for spectral functions obtained with the finite-temperature Lanczos method for finite two-dimensional clusters. Numerical results are additionally compared with the self consistent Born approximation (SCBA) results for hole-like (photoemission) and electron-like (inverse photoemission) spectra at $T = 0$. The analysis is suggesting that the origin of the pseudo gap is in short-range antiferromagnetic (AFM) spin correlations and strong asymmetry between the hole and electron spectra in the underdoped regime.

We analyze also the electron momentum distribution function (EMD). Our analytical results for a single hole in an AFM based on the SCBA indicate an anomalous momentum dependence of EMD showing "hole pockets" coexisting with a signature of an emerging large Fermi surface (FS). The position of the incipient FS and the structure of the EMD is determined by the momentum of the ground state. The main observation is the coexistence of two apparently contradicting FS scenarios. On the one hand, the δ-function like contributions at $(\pi/2, \pi/2)$ indicate, that for finite doping a pocket-like small FS evolves from these points, provided provided that AFM long range order persists. On the other hand, the discontinuity which appears at the same momentum is more consistent with with infinitesimally short arc (point) of an emerging large FS.

1. GENERALIZED t-J MODEL

Spectral properties of underdoped cuprates are of current interest, in particular results for the electron spectral functions as obtained with the angle resolved photoemission (ARPES) [1, 2, 3]. A remarkable feature of the ARPES data is the appearance of a pseudogap already at temperature T^* well above the superconducting T_c. Other quantities, e.g., the uniform susceptibility, the Hall constant and the specific heat also show a pseudogap consistent with energy scale T^* [4]. At very low temperature $T \ll T^*$ the Fermi surface and the corresponding electron spectral functions change dramatically with doping of planar cuprate systems with holes, where a transition from "small" to "large" FS seems to be consistent with ARPES, but is not adequately understood from the theoretical point of view.

There have been also several theoretical investigations of this problem, using the exact diagonalization (ED) of small clusters [5, 6, 7, 8], string calculations [9], slave-boson theory [10] and the high temperature expansion [11]. While a consensus has been reached about the existence of a large Fermi surface in the optimum-doped and overdoped materials, in the interpretation of ARPES experiments on *underdoped* cuprates the issue of the debate is (i) why are experiments more consistent with the existence of parts of a large FS – Fermi arcs or Fermi patches [3, 12] – rather than with a hole pocket type small FS, predicted by several theoretical methods based on the existence of AFM long range order in cuprates, (ii) how does a partial FS eventually evolve with doping into a large closed one.

The main emphasis of the present study is on the pseudo gap found in ARPES and also in some exact diagonalization studies [13, 14, 15]. We employ the standard t-J model to which we add a nearest neighbor repulsion term V,

$$\begin{aligned} H &= -t \sum_{<ij>,\sigma} (c^\dagger_{i,\sigma} c_{j,\sigma} + \text{H.c.}) + \\ &\quad + \sum_{<ij>} [J S^z_i S^z_j + \frac{\gamma}{2} J (S^+_i S^-_j + S^-_i S^+_j) + (V - \frac{J}{4}) n_i n_j]. \quad (1.1) \end{aligned}$$

Here i, j refer to planar sites on a square lattice and $c^\dagger_{is}$ represent projected fermion operators forbidding double occupation of sites. S^α_i are spin operators. For convenience we treat the anisotropy γ as a free parameter, with $\gamma = 0$ in the Ising case, and $\gamma \to 1$ in the Heisenberg model.

Numerical results presented here were obtained with Lanczos exact diagonalization (ED) technique on small clusters with $N = 16 \sim 32$ sites, for temperature in the range $T < J$. The method is simple: we take into account only the lowest ≈ 100 Lanczos states and evaluate the corresponding thermal averages. The method is compared with a more elaborate finite-temperature Lanczos method (FTLM) [13] and the agreement in here studied $T < J$ regime is excellent. It should be noted that for low temperatures the results of the diagonalization of small clusters always have to be examined with caution, because low energy scale exhibits very strong finite size effects.

Our analytical approach is based on a spinless fermion – Schwinger boson representation of the t-J Hamiltonian [16] and on the SCBA for calculating both the Green's function [16, 17, 18] and the corresponding wave function

[19, 20]. The method is known to be successful in determining spectral and other properties of the quasi particles (QP). In contrast to other methods the SCBA is expected to correctly describe the *long-wavelength* physics, the latter being determined by the linear dispersion of spin waves, whereas the *short-wavelength* properties can be studied with various other methods. Here we compare the SCBA results with the corresponding ED, as shown further-on.

In the SCBA fermion operators are decoupled into hole and pseudo spin – local boson operators: $c_{i,\uparrow} = h_i^\dagger$, $c_{i,\downarrow} = h_i^\dagger S_i^+ \sim h_i^\dagger a_i$ and $c_{i,\downarrow} = h_i^\dagger$, $c_{i,\uparrow} = h_i^\dagger S_i^- \sim h_i^\dagger a_i$ for i belonging to A- and B-sublattice, respectively. The effective Hamiltonian emerges

$$\tilde{H} = N^{-1/2} \sum_{\mathbf{kq}} (M_{\mathbf{kq}} h^\dagger_{\mathbf{k-q}} h_{\mathbf{k}} \alpha^\dagger_{\mathbf{q}} + \text{H.c.}) + \sum_{\mathbf{q}} \omega_{\mathbf{q}} \alpha^\dagger_{\mathbf{q}} \alpha_{\mathbf{q}}, \qquad (1.2)$$

where $h^\dagger_{\mathbf{k}}$ is the creation operator for a (spinless) hole in a Bloch state. The AFM boson operator $\alpha^\dagger_{\mathbf{q}}$ creates an AFM magnon with the energy $\omega_{\mathbf{q}}$, and $M_{\mathbf{kq}}$ is the fermion-magnon coupling.

We calculate the Green's function for a hole $G_{\mathbf{k}}(\omega)$ within the SCBA [16, 17, 18]. This approximation amounts to the summation of non-crossing diagrams to all orders and the corresponding ground state wave function with momentum $\mathbf{k}$ and energy $\epsilon_{\mathbf{k}}$ [19, 20, 21] is represented as

$$\begin{aligned} |\Psi_{\mathbf{k}}\rangle &= Z_{\mathbf{k}}^{1/2} \Big[h^\dagger_{\mathbf{k}} + \ldots + N^{-n/2} \sum_{\mathbf{q}_1,\ldots,\mathbf{q}_n} M_{\mathbf{k}\mathbf{q}_1} G_{\bar{\mathbf{k}}_1}(\bar{\omega}_1) \ldots M_{\bar{\mathbf{k}}_{n-1}\mathbf{q}_n} \times \\ &\qquad \times G_{\bar{\mathbf{k}}_n}(\bar{\omega}_n)\, h^\dagger_{\bar{\mathbf{k}}_n} \alpha^\dagger_{\mathbf{q}_1} \ldots \alpha^\dagger_{\mathbf{q}_n} + \; \ldots \; \Big] |0\rangle. \end{aligned} \qquad (1.3)$$

Here $\bar{\mathbf{k}}_m = \mathbf{k} - \mathbf{q}_1 - \ldots - \mathbf{q}_m$, $\bar{\omega}_m = \epsilon_{\mathbf{k}} - \omega_{\mathbf{q}_1} - \ldots - \omega_{\mathbf{q}_m}$ and $Z_{\mathbf{k}}$ is the QP spectral weight.

2. PSEUDO GAP IN THE DENSITY OF STATES

We study here the planar density of states (DOS), defined as $\mathcal{N}(\omega) = 2/N \sum_{\mathbf{k}} A_{\mathbf{k}}(\omega - \mu)$, where $A_{\mathbf{k}}(\omega)$ is the electron spectral function [14, 13], and μ denotes the chemical potential. First we calculate the DOS with the finite-temperature Lanczos method for clusters of $N = 18, 20$ sites doped with one hole, $N_h = 1$. Here we denote with $\mathcal{N}^-(\omega)$ the density of states corresponding to adding a hole into the system and thus to the photoemission experiments, while $\mathcal{N}^+(\omega)$ represents the inverse photoemission (IPES) spectra.

In Fig. 1.1(a) we present $\mathcal{N}(\omega)$ for two different $J/t = 0.3$ and $J/t = 0.6$ on a $N = 18$ sites cluster for $V = 0$. We observe that the pseudo gap scales approximately as $2J$. The analysis at elevated temperatures shows that the gap slowly fills up and disappears at $T \sim J$. In Fig. 1.1(b) results for different values V are presented. The gap remains robust also in the presence of the

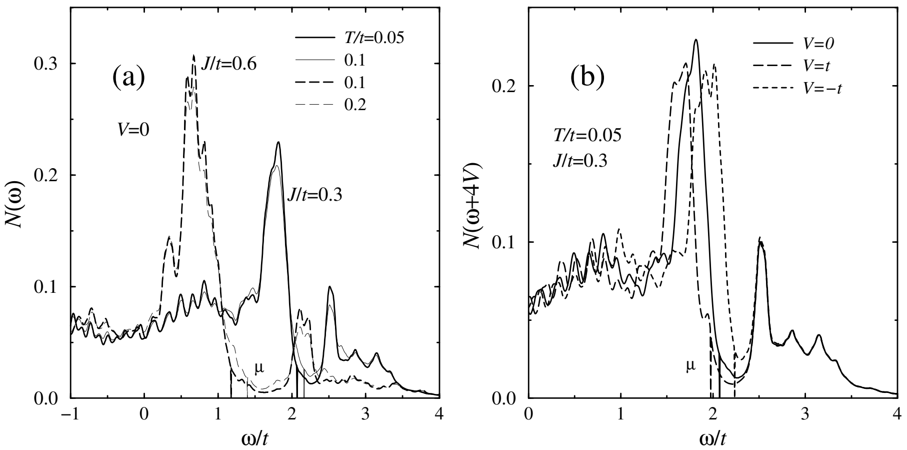

Figure 1.1 $\mathcal{N}(\omega)$ for one hole on $N = 18$ sites, presented for different J/t, V/t and T/t. (a) $V = 0$. (b) $J = 0.3t$. Broadening of peaks is taken $\delta/t = 0.04$.

V term, which enhances ($V < 0$) or suppresses ($V > 0$) the binding of hole pairs. It is thus evident that the effect of V is only of qualitative character and not relevant for the existence of the pseudo gap. We therefore believe that this analysis suggests that the origin of the pseudo gap is in short-range AFM spin correlations rather than in the binding tendency of doped holes.

AFM spin correlations are correctly taken into account in the SCBA. Therefore for the limiting case of low doping, $c_{\mathrm{h}} \to 0$, and $T \to 0$ we approximate $\mathcal{N}^-(\omega)$ with

$$\mathcal{N}^-(\omega) \propto \sum_{\mathbf{k}} \mathrm{Im} G_{\mathbf{k}}(-\omega), \tag{1.4}$$

where $G_{\mathbf{k}}(\omega)$ is the SCBA Green's function for adding one hole (ARPES) to an AFM reference system (instead of adding one hole to the state with one hole). The corresponding DOS for *removing* a hole (IPES) from the state with one hole, $\mathcal{N}^+(\omega) = \frac{2}{N}\sum_{\mathbf{k}} A^+_{\mathbf{k}}(\omega)$, can be calculated accurately in the SCBA as follows. First the spin averaged hole-like spectral function,

$$A^+_{\mathbf{k}}(\omega) = -\frac{1}{2\pi}\mathrm{Im}\sum_{\sigma}\langle\Psi_{\mathbf{k}_0}|c_{\mathbf{k},\sigma}\frac{1}{\omega-\tilde{H}}c^\dagger_{\mathbf{k},\sigma}|\Psi_{\mathbf{k}_0}\rangle, \tag{1.5}$$

is expressed in terms of holon and magnon operators and the result for $\mathcal{N}^+(\omega)$ emerges,

$$\mathcal{N}^+(\omega) = \frac{1}{N}\sum_{i}\langle\Psi_{\mathbf{k}_0}|h^\dagger_i[\delta(\omega-\tilde{H}) + a_i\delta(\omega-\tilde{H})a^\dagger_i]h_i|\Psi_{\mathbf{k}_0}\rangle. \tag{1.6}$$

Here $|\Psi_{\mathbf{k}_0}\rangle$ represents a weakly doped AFM, i.e., it is the ground state (GS) wave function of a planar AFM with one hole and the GS wave vector $\mathbf{k}_0$.

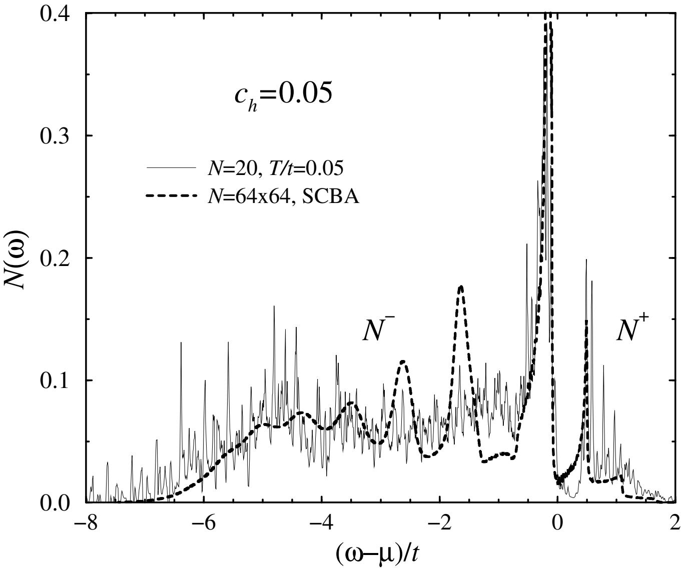

Figure 1.2 $\mathcal{N}(\omega)$ for $N_h = 1$ on $N = 20$ sites, with $J/t = 0.3$, $V = 0$, $T/t = 0.05$ (full line). Dashed heavy line represents the SCBA result on large lattice obtained as a sum of $\mathcal{N}^-(\omega)$ and $\mathcal{N}^+(\omega)$. The SCBA result is obtained on a $N = 64 \times 64$ cluster and for undoped reference system. Note the "string states" resonances, absent in the finite doping Green's function. $\mathcal{N}^+(\omega)$ corresponds to IPES. Reference hole concentration is $c_{\mathrm{h}} = 1/N$. The SCBA result is normalized to $c_{\mathrm{h}} = 1/20$. Broadening of peaks is taken $\delta/t = 0.01$.

The normalization (sum rule) of $A^{\pm}_{\mathbf{k}}(\omega)$ and $\mathcal{N}^{\pm}(\omega)$ is discussed in detail in Ref. [13]. It should be noted that the normalization of $A^{+}_{\mathbf{k}}(\omega)$ is not trivial and is related to the EMD presented in the next section.

In Fig. 1.2 are shown spectra $\mathcal{N}(\omega)$ obtained with the ED on a $N = 20$ sites cluster. We compare these spectra with the DOS within the SCBA. The peaks in $\mathcal{N}^+(\omega)$ can well be explained with magnon structure of single hole ground state, while peaks in $\mathcal{N}^-(\omega)$ are string states known in the single hole case and are for the present study of the pseudo gap and FS not relevant. As seen in Fig. 1.2 the total DOS obtained with the SCBA and in particular $\mathcal{N}^+(\omega)$ remarkably accurately resemble the ED DOS.

3. LARGE OR SMALL FERMI SURFACE?

The electron momentum distribution function $n_{\mathbf{k}} = \langle \Psi_{\mathbf{k}_0} | \sum_\sigma c^\dagger_{\mathbf{k},\sigma} c_{\mathbf{k},\sigma} | \Psi_{\mathbf{k}_0} \rangle$ is the key quantity for resolving the problem of the Fermi surface. Numerically $n_{\mathbf{k}}$ can be determined by exact diagonalization of the model in small clusters, where only a restricted number of momenta $\mathbf{k}$ is allowed. The GS wave vector due to finite size effects varies with N. Therefore we present here

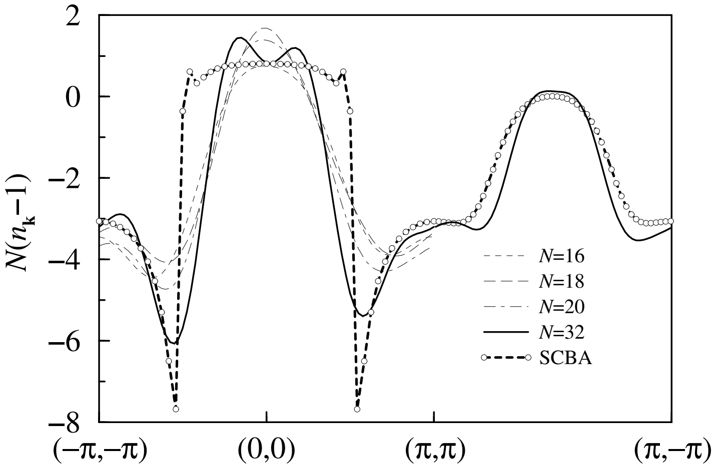

Figure 1.3 $N(n_{\mathbf{k}}-1)$ obtained from ED for various systems $N=16,18,20,32$ and $J/t=0.3$. For the SCBA $N=64\times 64$, $\gamma=0.999$ and note that delta-function contributions at $\mathbf{k}=\pm\mathbf{k}_0$ are not shown. In plotting the curve for $N=32$ data from Ref. [8] were used.

results obtained with the method of twisted boundary conditions [22], where $t_{jj'}\to t_{jj'}\exp i\theta_{jj'}$. Since $n_{\mathbf{k}}\equiv n_{\mathbf{k}}(\mathbf{k}_0,\theta)$ depends both on $\mathbf{k}_0$ and θ it follows from Peierls construction that $n_{\mathbf{k}}(\mathbf{k}_0,0)=n_{\mathbf{k}+\mathbf{k}_0}(0,\mathbf{k}_0)$ for $\theta=\mathbf{k}_0$. This allows us to study $n_{\mathbf{k}}$ for arbitrary $\mathbf{k}$ and $\mathbf{k}_0$. Furthermore, the finite size effects of the results are suppressed if we fix $\mathbf{k}_0$ for *all clusters* here studied to the symmetry point $\mathbf{k}_0=(\frac{\pi}{2},\frac{\pi}{2})$.

In Fig. 1.3 we present for $J/t=0.3$ ED results for clusters with different N and $\gamma=1$. The EMD obeys the sum rule $\sum_{\mathbf{k}}n_{\mathbf{k}}=N-1$ and, for the allowed momenta, the constraint $N(n_{\mathbf{k}}-1)\le 1$. We show here the quantity $N(n_{\mathbf{k}}-1)$, which for different N scales towards the same curve. Results are presented for some selected directions in the Brillouin zone (BZ) and should be averaged over all four possible ground state momenta when discussed, e.g., in connection with ARPES data.

Analytically we study the EMD again in the spinless fermion – Schwinger boson representation. The wave function Eq. (1.3) corresponds to the projected space of the model Eq. (1.1) and $n_{\mathbf{k}}=\langle\Psi_{\mathbf{k}_0}|\hat{n}_{\mathbf{k}}|\Psi_{\mathbf{k}_0}\rangle$ with the projected *electron* number operator $\hat{n}_{\mathbf{k}}=\sum_\sigma c^\dagger_{\mathbf{k},\sigma}c_{\mathbf{k},\sigma}$. Consistent with the SCBA approach, we decouple $\hat{n}_{\mathbf{k}}$ into hole and magnon operators,

$$\hat{n}_{\mathbf{k}}=\frac{1}{N}\sum_{ij}h_ih_j^\dagger\Big(\eta^+_{ij}[1+a_i^\dagger a_j(1-\delta_{ij})]+\eta^-_{ij}(a_i^\dagger+a_j)\Big), \qquad (1.7)$$

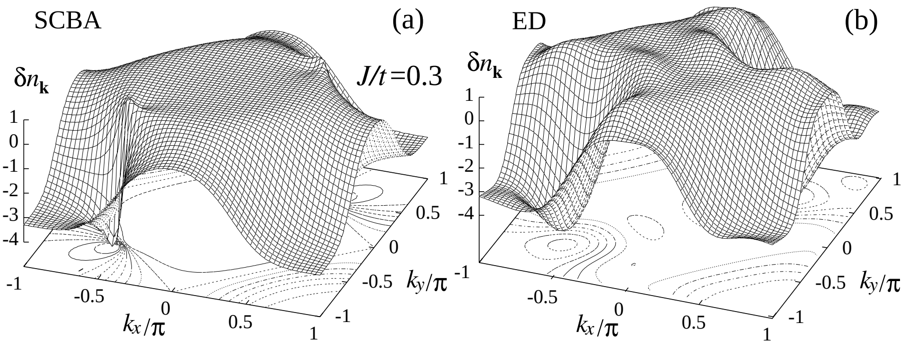

Figure 1.4 (a) SCBA result for $N = 64 \times 64$ and $J/t = 0.3$, $\gamma = 0.99$. (b) Exact diagonalization result for $N = 32$ sites as in Fig. 1.3.

where $\eta^{\pm}_{ij} = e^{-i\mathbf{k}\cdot(\mathbf{R}_i-\mathbf{R}_j)}(1 \pm e^{-i\mathbf{Q}\cdot(\mathbf{R}_i-\mathbf{R}_j)})/2$ with $\mathbf{Q} = (\pi, \pi)$. Local $a^\dagger_i$ are further expressed with proper magnon operators $\alpha^\dagger_{\mathbf{q}}$. In general the expectation value $n_{\mathbf{k}}$ for a single hole has the following structure [23]

$$n_{\mathbf{k}} = 1 - \frac{1}{2} Z_{\mathbf{k}_0}(\delta_{\mathbf{k}\mathbf{k}_0} + \delta_{\mathbf{k}\mathbf{k}_0+\mathbf{Q}}) + \frac{1}{N}\delta n_{\mathbf{k}}. \tag{1.8}$$

Here the second term proportional to δ-functions corresponds to hole pockets. Note that $\delta n_{\mathbf{k}}$, for the case of a single hole fulfills the sum rule $\frac{1}{N}\sum_{\mathbf{k}} \delta n_{\mathbf{k}} = Z_{\mathbf{k}_0} - 1$ and $\delta n_{\mathbf{k}} \leq 1$. The introduction of $\delta n_{\mathbf{k}}$ is convenient as it allows the comparison of results obtained with different methods and on clusters of different size N.

In Fig. 1.3 we also present the SCBA result. We have also checked the convergence of $\delta n_{\mathbf{k}}$ with the number of magnon lines, n. For $J/t > 0.3$ we find for all $\mathbf{k}$ that the contribution of terms $n > 3$ amounts to less than few percent. This is in agreement with the convergence of the norm of the wave function, which is even faster [20].

In Fig. 1.4(a) we present this $\delta n_{\mathbf{k}}$ for the whole BZ. The important ingredient of the SCBA is the gapless magnons with linear dispersion and a more complex ground state of the planar AFM. $G_{\mathbf{k}}(\omega)$ and $\epsilon_{\mathbf{k}}$ are strongly $\mathbf{k}$-dependent. As a consequence $n_{\mathbf{k}}$ in general depends both on $\mathbf{k}$ and $\mathbf{k}_0$. The ground state is for the t-J model fourfold degenerate and we again choose $\mathbf{k}_0 = (\frac{\pi}{2}, \frac{\pi}{2})$. In Fig. 1.4(b) is presented also the result of exact diagonalization of a $N = 32$ sites cluster [8], but generalized to the whole BZ.

The main conclusion regarding the EMD is the coexistence of two apparently contradicting Fermi-surface scenarios in EMD of a single hole in an AFM. (i) On one hand, the δ-function contributions in Eq. (1.8) seem to indicate that at finite doping a delta-function might develop into small Fermi surface, i.e., a hole pocket, provided that AFM long range order persists. (ii) A novel feature is that also $\delta n_{\mathbf{k}}$ is singular in a particular way, i.e., it shows a discontinuity at $\mathbf{k} = \mathbf{k}_0$ with a strong asymmetry with respect to $\mathbf{k}_0$. It is therefore more consistent with infinitesimally short arc (point) of an emerging large FS. For finite doping the discontinuity could possibly extend into such a finite arc (not closed) FS. Note that as long-range AFM order is destroyed by doping, hole pocket contributions should disappear while the singularity in $\delta n_{\mathbf{k}}$ could persist. The results of the two methods, the SCBA and the ED agree quantitatively at all points in the BZ. However, the SCBA result is *symmetric* around Γ point in the direction $\mathbf{k} \parallel \mathbf{k}_0$, while small system results show a weak asymmetry for $\mathbf{k} = \pm\mathbf{k}_0$, respectively. From our analysis of the SCBA results for $N \to \infty$ and long range AFM spin background it follows that in the thermodynamic limit $c_{\mathrm{h}} \to 0$ $n_{\mathbf{k}}$ is symmetric. The asymmetry is in Ref. [8] attributed to the opening of the gap in the magnon spectrum at $\mathbf{q} \sim \mathbf{Q}$ in finite systems. Within the SCBA the asymmetry also appears if the EMD is evaluated with $\mathbf{k}_0$ *displaced* from $(\frac{\pi}{2}, \frac{\pi}{2})$ by a small amount $\delta\mathbf{k}_0$ (not shown here).

4. SUMMARY AND ANALYTICAL RESULTS

Full numerical results are captured with a simple analytical expansion which gives more insight into the structure of $A^+_{\mathbf{k}}(\omega)$ and $\delta n_{\mathbf{k}}$. We simplify the wave function, Eq. (1.3), by keeping only the one-magnon contributions and take $J/t \gg 1$ and the leading order contributions are then

$$\begin{aligned}
A^+_{\mathbf{k}}(\omega) &\sim A^{(1)}_{\mathbf{k}}(\omega) = [Z_{\mathbf{k}_0}\delta_{\mathbf{q},0} + \frac{1}{N}(1 - \delta n^{(1)}_{\mathbf{k}})]\delta(\omega - \omega_{\mathbf{q}}), \\
\delta n^{(1)}_{\mathbf{k}} &= -Z_{\mathbf{k}_0} M_{\mathbf{k}_0\mathbf{q}} G_{\mathbf{k}_0}(\epsilon_{\mathbf{k}_0} - \omega_{\mathbf{q}})[2u_{\mathbf{q}} + M_{\mathbf{k}_0\mathbf{q}} G_{\mathbf{k}_0}(\epsilon_{\mathbf{k}_0} - \omega_{\mathbf{q}})] \\
&\sim -8Z^2_{\mathbf{k}_0} J \frac{\mathbf{q}\cdot\mathbf{v}}{\omega^2_{\mathbf{q}}}(1 + Z_{\mathbf{k}_0}\frac{\mathbf{q}\cdot\mathbf{v}}{\omega_{\mathbf{q}}}), \qquad q \to 0, \qquad (1.9)
\end{aligned}$$

with $\mathbf{q} = \mathbf{k} - \mathbf{k}_0$ (or $\mathbf{k} - \mathbf{k}_0 - \mathbf{Q}$) and $\mathbf{v} = t(\sin k_{0x}, \sin k_{0y})$.

A surprising observation is that the EMD exhibits for momenta $\mathbf{k} \sim \mathbf{k}_0, \mathbf{k}_0 + \mathbf{Q}$ a discontinuity $\sim Z_{\mathbf{k}_0} N^{1/2}$ and $\delta n^{(1)}_{\mathbf{k}} \propto -(1 + \mathrm{sign}\, q_x)/q_x$. These discontinuities are consistent with ED results. One can interpret this result as an indication of an emerging *large* Fermi surface at $\mathbf{k} \sim \pm\mathbf{k}_0$. The discontinuity appears only as *points* $\pm\mathbf{k}_0$, not *lines* in the BZ. Note, however, that this result is obtained in the extreme low doping limit, i.e., $c_{\mathrm{h}} = 1/N$ and it is not straightforward to generalize it to the finite doping regime.

A direct reflection of the anomaly in $\delta n_{\mathbf{k}}$ is also the structure of $A_{\mathbf{k}}(\omega)$ as presented in Fig. 1.5(a), where $A^+_{\mathbf{k}}(\omega)$ exhibits a typical asymmetry in momentum dependence. This shows the instability towards the large FS. The electron part is in this figure approximated with $A^-_{\mathbf{k}}(\omega) \sim Z_{\mathbf{k}_0}\delta(\epsilon_{\mathbf{k}} - \epsilon_{\mathbf{k}_0} - \omega)$. In Fig. 1.5(b) $\delta n^{(1)}_{\mathbf{k}}$ is presented and the anomaly discussed above is clearly seen.

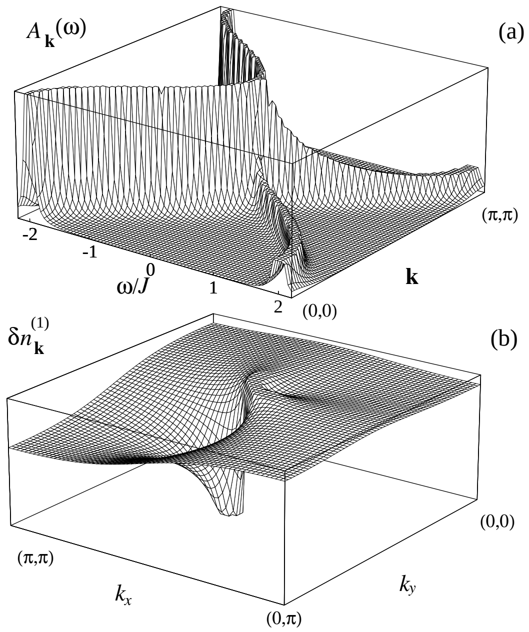

Figure 1.5 The tendency of formation of the large FS as seen in (a) $A_{\mathbf{k}}(\omega)$ and (b) $\delta n^{(1)}_{\mathbf{k}}$ for $Z_{\mathbf{k}_0} t/J \sim 1$. The figures are in arbitrary units and clipped for convenience.

We conclude by stressing that the origin of the pseudo gap found in cuprates seems to be in the short range spin correlations of the reference AFM system, as well as in the strong asymmetry between the hole-like and electron-like spectra in underdoped systems. From the present SCBA analysis it is clear that the gap size is a natural consequence of magnons with dispersion $\sim 2J$, and the first peak in $\mathcal{N}^{+}(\omega)$ thus corresponds to the "van Hove" high density of magnon states. In addition in making contact with ARPES experiments we should note that ARPES measures the imaginary part of the electron Green's function. We must note that using these experiments in underdoped cuprates $n_{\mathbf{k}}$ can be only qualitatively discussed since the latter is extracted only from rather restricted frequency window below the chemical potential. Nevertheless our results are not consistent with a small hole pocket FS (at least only a part of presumable closed FS is visible), but rather with partially developed arcs resulting in FS which is just a set of disconnected segments at low temperature collapsing to the point [1, 3]. The SCBA results for singular $\delta n_{\mathbf{k}}$ seem to allow for such a scenario. It should also be stressed that the SCBA approach is based on the AFM long-range order, still we do not expect that finite but longer-range AFM correlations would entirely change our conclusions.

References

[1] J.C. Campuzano and M. Randeria, this volume, p. 11.

[2] Z.-X. Shen and D.S. Dessau, Phys. Rep. **253**, 1 (1995); B.O. Wells *et al.*, Phys. Rev. Lett. **74**, 964 (1995); D.S. Marshall *et al.*, Phys. Rev. Lett. **76**, 4841 (1996).

[3] M.R. Norman *et al.*, Nature **392**, 157 (1998).

[4] For a review see, e.g., M. Imada, A. Fujimori, and Y. Tokura, Rev. Mod. Phys. **70**, 1039 (1998).

[5] For a review see, e.g., E. Dagotto, Rev. Mod. Phys. **66**, 763 (1994).

[6] W. Stephan and P. Horsch, Phys. Rev. Lett. **66**, 2258 (1991).

[7] R. Eder and Y. Ohta, Phys. Rev. B **57**, R5590 (1998).

[8] A.L. Chernyshev, P.W. Leung and R.J. Gooding, Phys. Rev. B **58**, 13594 (1998).

[9] R. Eder, Phys. Rev. B, **44**, R12609 (1991).

[10] X.-G. Wen and P.A. Lee, Phys. Rev. Lett. **76**, 503 (1996).

[11] W.O. Putikka, M.U. Luchini, and R.R.P. Singh, J. Phys. Chem. Solids **59**, 1858 (1998); Phys. Rev. Lett. **81**, 2966 (1998).

[12] N. Furukawa, T.M. Rice, and M. Salmhofer, Phys. Rev. Lett., **81**, 3195 (1998).

[13] For a review see J. Jaklič and P. Prelovšek, Adv. Phys. **49**, 1 (2000).

[14] P. Prelovšek, J. Jaklič, and K. Bedell, Phys. Rev. B **60**, 40 (1999).

[15] P. Prelovšek, A. Ramšak, and I. Sega, Phys. Rev. Lett. **81**, 3745 (1998).

[16] S. Schmitt-Rink, C.M. Varma, and A.E. Ruckenstein, Phys. Rev. Lett. **60**, 2793 (1988).

[17] A. Ramšak and P. Prelovšek, Phys. Rev. B **42**, 10415 (1990).

[18] G. Martínez and P. Horsch, Phys. Rev. B **44**, 317 (1991).

[19] G.F. Reiter, Phys. Rev. B **49**, 1536 (1994).

[20] A. Ramšak and P. Horsch, Phys. Rev. B **48**, 10559 (1993); *ibid.* **57**, 4308 (1998).

[21] J. Bała, A. M. Oleś, and J. Zaanen, Phys. Rev. B **52**, 4597 (1995).

[22] X. Zotos, P. Prelovšek and I. Sega, Phys. Rev. B **42**, 8445 (1990).

[23] A. Ramšak, P. Prelovšek, and I. Sega, Phys. Rev. B **61**, 4389 (2000).